Zuse Institute Berlin

Takustr. 7
14195 Berlin
Germany

FELIX AMBELLAN[1], STEFAN ZACHOW[2],
CHRISTOPH VON TYCOWICZ[3]

A Surface-Theoretic Approach for Statistical Shape Modeling[4]

[1] 0000-0001-9415-0859, corresponding author
[2] 0000-0001-7964-3049
[3] 0000-0002-1447-4069
[4] to appear in: Medical Image Computing and Computer Assisted Intervention (MICCAI)

{ambellan, zachow, vontycowicz}@zib.de

Zuse Institute Berlin
Takustr. 7
14195 Berlin
Germany

Telephone: +49 30-84185-0
Telefax: +49 30-84185-125

E-mail: bibliothek@zib.de
URL: http://www.zib.de

ZIB-Report (Print) ISSN 1438-0064
ZIB-Report (Internet) ISSN 2192-7782

A Surface-Theoretic Approach for Statistical Shape Modeling

Felix Ambellan[0000−0001−9415−0859], Stefan Zachow[0000−0001−7964−3049], and Christoph von Tycowicz[0000−0002−1447−4069]

Therapy Planning Group, Zuse Institute Berlin, Berlin, Germany
{ambellan, zachow, vontycowicz}@zib.de

Abstract. We present a novel approach for nonlinear statistical shape modeling that is invariant under Euclidean motion and thus alignment-free. By analyzing metric distortion and curvature of shapes as elements of Lie groups in a consistent Riemannian setting, we construct a framework that reliably handles large deformations. Due to the explicit character of Lie group operations, our non-Euclidean method is very efficient allowing for fast and numerically robust processing. This facilitates Riemannian analysis of large shape populations accessible through longitudinal and multi-site imaging studies providing increased statistical power. We evaluate the performance of our model w.r.t. shape-based classification of pathological malformations of the human knee and show that it outperforms the standard Euclidean as well as a recent nonlinear approach especially in presence of sparse training data. To provide insight into the model's ability of capturing natural biological shape variability, we carry out an analysis of specificity and generalization ability.

Keywords: Statistical shape analysis · Principal geodesic analysis · Lie groups · Classification · Manifold valued statistics

1 Introduction

Statistical shape models (SSMs) have become an essential tool for medical image analysis with a wide range of applications such as segmentation of anatomical structures, computer-aided diagnosis, and therapy planning. SSMs describe the geometric variability in a population in terms of a mean shape and a hierarchy of major modes explaining the main trends of shape variation. Based on a notion of shape space, SSMs can be learned from a database of consistently parametrized instances from the object class under study. The resulting models provide a shape prior that can be used to constrain synthesis and analysis problems. Moreover, their parameter space provides a compact representation that is amenable to learning algorithms (e.g. classification or clustering), evaluation, and exploration.

Standard SSMs treat the space of shapes as a Euclidean vector space allowing for linear statistics to be applied (see e.g. [22] and the references therein). Linear methods, however, are often inadequate for capturing the high variability in biological shapes [12]. Nonlinear approaches have been developed based

on geometric as well as physical concepts such as Hausdorff distance [8], elasticity [25, 27, 28], and viscous flows [17, 6, 20]. In general, these methods lack numerical robustness and fast response rates limiting their practical applicability especially in interactive applications. To address these challenges, one line of work models shapes by a collection of primitives [14, 16, 21] that naturally belong to Lie groups and effectively describe local changes in shape. Performing intrinsic calculus on the uncoupled primitives allows for fast computations while, at the same time, accounting for the nonlinearity in shape variation. However, solving the inverse problem, i.e. mapping from primitives back to surface meshes, is generally non-trivial. Recently, von Tycowicz et al. [26] presented a physically motivated approach based on differential coordinates for which the inverse problem is well-known and can be solved at linear cost. Despite their inherent nonlinear structure, the employed representations are not invariant under Euclidean motion and, thus, suffer from bias due to arbitrary choices. While the effect of rigid motions can be removed between pairs of shapes using alignment strategies, non-transitivity thereof prevents true group-wise alignment.

This work presents a novel shape representation based on discrete fundamental forms that is invariant under Euclidean motion. We endow this representation with a Lie group structure that admits bi-invariant metrics and therefore allows for consistent analysis using manifold-valued statistics based on the Riemannian framework. Furthermore, we derive a simple, efficient, robust, yet accurate (i.e. without resorting to model approximations) solver for the inverse problem that allows for interactive applications.

Although in computer graphics and vision communities, rotation invariant differential coordinates have also been successfully employed for geometry processing applications, e.g. [24, 19, 18], these approaches fall short of a fully intrinsic treatment (e.g. due to lack of bi-invariant group structure and linearization) and have not been adapted to the field of SSMs.

2 Rotation Invariant Surface Representation

In this section, we derive a discrete surface representation based on concepts from differential geometry of smooth surfaces.

Relation to Surface Theory To every smooth surface there uniquely exist two smoothly pointwise varying and symmetric bilinear forms on the tangent plane, the so called *fundamental forms*. The *first* fundamental form I (a.k.a. metric tensor) is positive definite and allows for angle, length and area measurement. The *second* fundamental form II describes the curvature of the surface. A prominent result in classical mathematics, the *Fundamental Theorem of Surface Theory* due to Bonnet ($\approx$1860, e.g. [7] Sec. 4.3), states that if given two symmetric bilinear forms (one of them positive definite), s.t. for both certain integrability conditions hold (viz. the Gauß–Codazzi equations), then they (locally) determine uniquely, up to global rotation and translation, a surface embedded in three dimensional space with these two as its fundamental forms. Therefore, a discrete description of the fundamental forms is an excellent candidate for a

rotation-invariant surface representation. In the following, we will denote our proposed shape model as the *fundamental coordinate model* (FCM).

Discretization We consider shapes that belong to a particular population of anatomical structures, s.t. each digital shape S can be described as a left-acting deformation ϕ of a common reference shape $\bar{S}$ given as triangulated surface. Let deformation ϕ be affine on each triangle $\bar{T}_i$ of $\bar{S}$, then the deformation gradient $\nabla\phi$ is the 3×3 matrix of partial derivatives of ϕ and constant on each triangle $D_i := \nabla\phi|_{\bar{T}_i}$ (see e.g. [5] for detailed expressions). Assuming ϕ to be an orientation-preserving embedding of $\bar{S}$, we can decompose D_i uniquely into its rotational R_i and stretching U_i components by means of the polar decomposition $D_i = R_i U_i$. Note that U_i furnishes a complete description of the metric distortion of $\bar{T}_i$ and is defined in reference coordinates, hence invariant under rotation of S. Indeed, we can obtain a representation of the first fundamental form by restricting the stretches to the tangent plane. To this end, we define an arbitrary but fixed element-wise field $\{\bar{F}_i\}$ of orthonormal frames on $\bar{S}$, s.t. the last column of each frame is the normal of the respective element. Then, we represent the metric in terms of reduced stretch $\tilde{U}_i := [\bar{F}_i^T U_i \bar{F}_i]_{3,3} = \mathrm{I}|_{\bar{T}_i}^{1/2}$, where $[\,\cdot\,]_{3,3}$ denotes the submatrix with the third row and column removed.

As for the second fundamental form, we note that at a point $p \in S$ it is determined by the differential of the normal field N, viz. $\mathrm{II}_p(v, w) = \mathrm{I}_p(-dN_p(v), w)$ for tangent vectors v, w. For a triangulated surface, the differential dN is supported along the edges. In order to derive a representation thereof, we induce the frame field $\{F_i\}$ on S consistent to $\{\bar{F}_i\}$ using the rotational part of the deformation gradient, i.e. $F_i = R_i \bar{F}_i$. This allows us to define *transition rotations* $F_i C_{ij} = F_j$ for each inner edge (incident to triangles T_i, T_j) that fully describe the change in normal directions. Note that, while both the frames $\{F_i\}$ and the rotations $\{R_i\}$ are equivariant, the transition rotations $\{C_{ij}\}$ are invariant under global rotations of S and $\bar{S}$.

Group Structure In order to perform intrinsic statistical analysis, we derive a distance that is compatible with the underlying representation space. In particular, we endow the space with a Lie group structure together with a bi-invariant Riemannian metric for which group and Riemannian notions of exponential and logarithm coincide. This allows us to exploit closed-form expressions to perform geodesic calculus yielding simple, efficient, and numerically robust algorithms. We recommend chapter two of [1] to readers interested in deeper insight about bi-invariant metrics on Lie groups. This regards especially their existence and the geometric consequences thereof.

Our shape representation consists of transition rotations $C_{ij} \in \mathrm{SO}(3)$ (one per inner edge) and tangential stretches $\tilde{U}_i \in \mathrm{Sym}^+(2)$ (one per triangle), where $\mathrm{SO}(3)$ is the Lie group of rotations in $\mathbb{R}^3$ and $\mathrm{Sym}^+(2)$ the space of symmetric and positive definite 2×2 matrices. Following the approach in [3], we equip $U, V \in \mathrm{Sym}^+(2)$ with a multiplication $U \circ V := \exp(\log(U) + \log(V))$, s.t. $\mathrm{Sym}^+(2)$ turns into a commutative Lie group. It now allows for a bi-invariant metric induced by the Frobenius inner product yielding distance $d_{\mathrm{Sym}^+(2)}(U, V) = \|\log(V) - \log(U)\|_2$. $\mathrm{SO}(3)$ also admits a bi-invariant metric induced by the

Frobenius inner product with distance $d_{\mathrm{SO}(3)}(Q,R) = \left\|\log(Q^T R)\right\|_2$, s.t. we define our representation space as the product group $G := \mathrm{SO}(3)^n \times \mathrm{Sym}^+(2)^m$ and m, n the number of triangles and inner edges. Finally, we define the distance of $S, T \in G$ as

$$d(S,T) = \frac{\omega^3}{\bar{A}_{\mathcal{E}}} \sum_{(i,j)\in\mathcal{E}} \bar{A}_{ij}\, d_{\mathrm{SO}(3)}\left(C_{ij}^S, C_{ij}^T\right) + \frac{\omega}{\bar{A}} \sum_{i=1}^{m} \bar{A}_i\, d_{\mathrm{Sym}^+(2)}\left(\tilde{U}_i^S, \tilde{U}_i^T\right),$$

where $\omega \in \mathbb{R}^+$ is a weighting factor, $\mathcal{E}$ is the set of inner edges, $\bar{A}_i$ is the area of triangle $\bar{T}_i$, $\bar{A}_{ij} = 1/3(\bar{A}_i + \bar{A}_j)$, $\bar{A}_{\mathcal{E}} = \sum_{(i,j)\in\mathcal{E}} \bar{A}_{ij}$, and $\bar{A} = \sum_{i=1}^m \bar{A}_i$. Here the area terms provide invariance under refinement of the mesh as well as simultaneous scaling of $\bar{S}, S, T$, whereas ω allows for commensuration of the curvature and metric contributions inspired by the Koiter thin shell model (e.g. [9] Sec. 4.1).

Model construction The derived representation carries a rich non-Euclidean structure calling for manifold-valued generalizations for first and second moment statistical analysis. To this end, we employ Principal Geodesic Analysis (PGA) [15]. Furthermore, to avoid systematic bias due to the choice of reference shape $\bar{S}$, we require it to agree with the mean of the training data as proposed in [23].

3 Efficient Numerics

In this section, we derive an efficient numerical solver for the inverse problem of mapping a point in representation space G to a corresponding shape $S = \phi(\bar{S})$. If the corresponding rotations $\{R_i\}$ were known, ϕ could be obtained as the minimizer of $\sum_{i=1}^m \bar{A}_i \left\|D_i - R_i U_i\right\|_2^2$ by solving the well-known Poisson equation (see e.g. [5, 26]). However, in our representation the rotations are only given implicitly in terms of the transition rotations. In particular, an immediate computation shows that $R_j = R_i \bar{F}_i C_{ij} \bar{F}_j^T =: R_{i\to j}$ for an integrable field $\{C_{ij}\}$. Based on this condition, for each triangle T_i we can formulate a residual term $\varepsilon_i(\phi, \{R_i\}) = \sum_{j\in\mathcal{N}_i} 1/|\mathcal{N}_i| \left\|D_i - R_{j\to i} U_i\right\|_2^2$ in terms of the rotations of neighboring triangles (indexed by $\mathcal{N}_i$). Then, the objective for the inverse problem is given as $E(\phi) = \min_{\{R_i\in\mathrm{SO}(3)\}} E(\phi, \{R_i\})$, where $E(\phi, \{R_i\}) = \sum_{i=1}^m \bar{A}_i\, \varepsilon_i(\phi, \{R_i\})$. Although $E(\phi)$ is a nonlinear function calling for iterative optimization routines, it exhibits a special structure amenable to an efficient alternating minimization technique. Specifically, we employ a block coordinate descent strategy that alternates between a local and a global step:

Local step: First, we minimize $E(\phi, \{R_i\})$ over the rotations $\{R_i\}$ keeping ϕ (hence D_i) fixed. Each summand in ε_i depends on a single rotation R_j, s.t. the problem decouples into individual low-dimensional optimizations that can be solved in closed-form and allow for massive parallelization.

Global step: Second, we minimize $E(\phi, \{R_i\})$ over ϕ with rotations $\{R_i\}$ fixed leading to a quadratic optimization problem for which the optimally conditions are determined by a Poisson equation. As the system matrix is sparse and depends only on the reference shape, it can be factorized once during the preprocess allowing for very efficient global solves with close to linear cost.

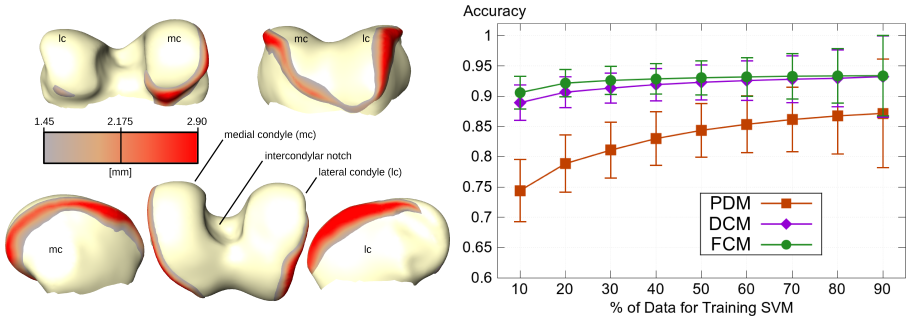

Fig. 1. Left: Mean shape of healthy distal femora overlaid with mean shape of the diseased femora wherever the distance is larger than 1.45mm, colored accordingly. Right: OA classification experiment for the proposed FCM, PDM [10] and DCM [26].

Note that the objective is bounded from below and that both local and global steps feature unique solutions that are guaranteed to weakly decrease the objective making any numerical safeguards unnecessary. This contrasts with classical approaches that require precautions, such as line search strategies and modification schemes for singular or indefinite Hessians, to guarantee robustness.

Initialization To provide the solver with a warm start, we compute an initial guess for the rotation field $\{R_i\}$. To this end, we employ the local integrability condition $R_j = R_{i\to j}$ to propagate an initial rotation matrix from an arbitrary seed along a precomputed spanning tree of the dual graph of $\bar{S}$. Note, that this strategy recovers the rotation field exactly for integrable $\{C_{ij}\}$. In case of non-integrable fields, one advantage of the Poisson-based reconstruction (global step) is that it distributes errors uniformly s.t. local inconsistencies are attenuated.

4 Experiments and Results

All experiments are performed employing a fixed commensuration weight $\omega = 10$ that empirically shows the best performance in our classification experiments (cf. suppl. material).

Data We employ three datasets: (i) Distal femora (see Fig. 1, left) from the Osteoarthritis Initiative (OAI) for 58 severely diseased and 58 healthy subjects that were also used for evaluation in [26] and are publicly available as segmentations [2], (ii) a male human body in two poses from the open-access FAUST [4] dataset (see Fig. 2, left) and (iii) synthetic pipe surfaces in a cylindrical and a helical configuration (see Fig. 2, right). For the former two, we used the surface meshes as provided by the authors (in particular the correspondences) and we refer to [4] and [26] for further details. A detailed list of the exact subjects that are included in (i) as well as their disease state can be found in the supplemental material.

Knee Osteoarthritis Classification Osteoarthritis (OA) is a degenerative disease of the joints that is i.a. characterized by changes of the bone shape (see

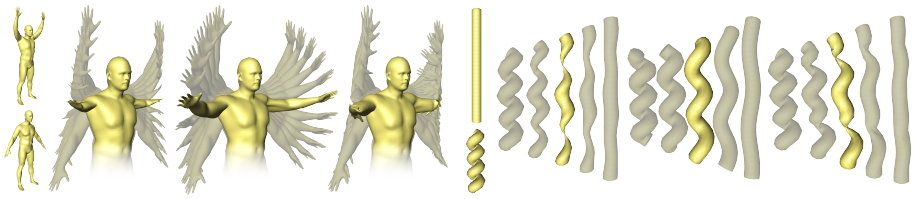

Fig. 2. Interpolating geodesic (mean highlighted) for the FAUST (left) and pipe surface (right) data within (f.l.t.r.) the PDM [10], the proposed FCM, and DCM [26], each.

Fig. 1, left). Here, we investigate the proposed FCM's ability to classify knee OA for the OAI dataset of distal femora. To this end, we employ a support vector machine (SVM) with linear kernel on the 115-dimensional feature vectors comprising the coefficients w.r.t. the principal modes for each shape. The classifier is trained on a balanced set of feature vectors for different shares of data varying from 10% to 90% with testing on the respective complement. To address the randomness of our experimental design, we carried out the experiment 10000 times per partition. We compare to the popular *point distribution model* [10] (PDM) as well as to the differential coordinates model [26] (DCM), which recently achieved highly accurate classification results. Figure 1 (right) shows the results in terms of average accuracy and standard deviation. Note that solely the FCM achieves an accuracy of over 90% in case of sparse (10%) training data.

Validity Frequently, datasets feature a high nonlinear variability that are characterized by large rotational components, which are insufficiently captured by linear models like PDM. While DCM treats the rotational components explicitly, it requires them to be well-localized, s.t. the logarithm is unambiguous. This assumption may not be satisfied for data with large spread in shape space. Contrary, our model overcomes this limitation utilizing a relative encoding: Transition rotations will never exceed 180° in practical scenarios (cf. supplemental material for a quantitative evaluation). In Fig. 2 we illustrate the validity of our model for two extreme examples in comparison to PDM and DCM.

Computational Performance We compare our framework in terms of performance to the state-of-the-art approaches: The *large deformation diffeomorphism metric mapping* (LDDMM) using the open-source Deformetrica [13] software, and the recent DCM. To this end, we compute the mean shape on 100 randomly sampled pairs from the OAI dataset. Overall, the LDDMM approach requires 172.8s (±44.8s) in average whereas the proposed FCM features an average runtime of only 2.3s (±1.9s), hence a two orders of magnitude speedup. In comparison to the highly efficient DCM—requiring 1.1s (±0.3s) in average—our model achieves runtimes within the same order of magnitude, despite the added nonlinearity in the inverse problem.

Specificity, Generalization Ability, Compactness We perform a quantitative comparison with PDM and DCM using standard measures (detailed in [11]) w.r.t. a physically-based surface distance $\mathcal{W}$ [20] as proposed in [26]. *Speci-*

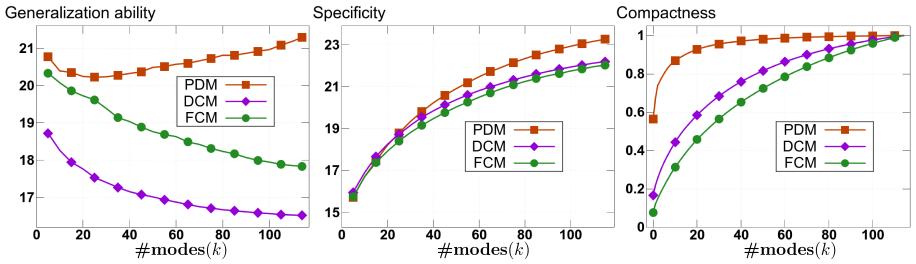

Fig. 3. Generalization ability (left), specificity (middle) and compactness (right) of the proposed FCM, PDM [10], and DCM [26].

ficity (Fig. 3 middle) evaluates the validity of the model generated instances in terms of their distance to the training shapes. We estimate it using 1000 randomly generated instances according to the distribution estimated by the respective model. *Generalization ability* (Fig. 3 left) assesses how well a model represents unseen instances. It is calculated in a leave-one-out study. *Compactness* (Fig. 3 right) measures the relative amount of variability of the training set captured by every mode in an accumulated manner. The results show that the FCM is more specific than PDM and DCM. In terms of generalization ability, the FCM is superior to PDM, yet inferior to DCM. Finally, the FCM is less compact than PDM and DCM. Note that compactness is calculated for each model w.r.t its own metric, hence not directly comparable. In particular, we found that decreasing ω leads to increased compactness, albeit at the expense of classification accuracy (cf. suppl. material). Therefore, we conjecture that lower compactness allows for more expressiveness within the different modes of variation.

5 Conclusion

In this work, we presented a novel nonlinear SSM based on a Euclidean motion invariant—hence alignment-free—shape representation with deep foundations in surface theory. The rich structure of the derived shape space assures valid shape instances even in presence of strong nonlinear variability. We perform manifold-valued statistics in a consistent Lie group setup allowing for closed-form evaluation of Riemannian operations. We show that this model yields highly discriminative shape descriptors that are superior to the state-of-the-art model [26] in experiments on OA classification. Furthermore, we devise an efficient and robust algorithm to solve the inverse problem that does not require any numerical safeguards. One possible and interesting way to proceed in the future is to replace the log-Euclidean metric with the affine-invariant one, which can be considered the natural metric on the symmetric positive definite matrices.

Acknowledgments

The authors are funded by the Deutsche Forschungsgemeinschaft (DFG, German Research Foundation) under Germany's Excellence Strategy – The Berlin Mathematics Research Center MATH+ (EXC-2046/1, project ID: 390685689). Furthermore we are grateful for the open-access datasets OAI [1] and FAUST [4] as well as for the open-source software Deformetrica [13].

References

1. Alexandrino, M.M., Bettiol, R.G.: Lie groups and geometric aspects of isometric actions, vol. 8. Springer (2015)
2. Ambellan, F., Tack, A., Ehlke, M., Zachow, S.: Automated segmentation of knee bone and cartilage combining statistical shape knowledge and convolutional neural networks. Med Image Anal **52**, 109–118 (2019)
3. Arsigny, V., Fillard, P., Pennec, X., Ayache, N.: Log-Euclidean metrics for fast and simple calculus on diffusion tensors. Magn Reson Med **56**(2), 411–421 (2006)
4. Bogo, F., Romero, J., Loper, M., Black, M.J.: FAUST: Dataset and evaluation for 3D mesh registration. In: CVPR. IEEE (2014)
5. Botsch, M., Sumner, R., Pauly, M., Gross, M.: Deformation transfer for detail-preserving surface editing. In: VMV. pp. 357–364 (2006)
6. Brandt, C., von Tycowicz, C., Hildebrandt, K.: Geometric flows of curves in shape space for processing motion of deformable objects. Comput Graph Forum **35**(2) (2016)
7. do Carmo, M.P.: Differential geometry of curves and surfaces. Prentice-Hall (1976)
8. Charpiat, G., Faugeras, O., Keriven, R., Maurel, P.: Distance-based shape statistics. In: ICASSP. pp. V925–V928. IEEE (2006)
9. Ciarlet, P.G.: An introduction to differential geometry with applications to elasticity. Journal of Elasticity **78**(1), 1–215 (Jan 2005)
10. Cootes, T.F., Taylor, C.J., Cooper, D.H., Graham, J.: Active shape models-their training and application. Comput Vis Image Underst **61**(1), 38–59 (1995)
11. Davies, R., Twining, C., Taylor, C.: Statistical Models of Shape: Optimisation and Evaluation. Springer (2008)
12. Davis, B.C., Fletcher, P.T., Bullitt, E., Joshi, S.: Population shape regression from random design data. Int J Comput Vis **90**(2), 255–266 (2010)
13. Durrleman, S., Prastawa, M., Charon, N., Korenberg, J.R., Joshi, S., Gerig, G., Trouvé, A.: Morphometry of anatomical shape complexes with dense deformations and sparse parameters. NeuroImage **101**(0), 35 – 49 (2014)
14. Fletcher, P.T., Lu, C., Joshi, S.: Statistics of shape via principal geodesic analysis on lie groups. In: CVPR. vol. 1, pp. I–95. IEEE (2003)

[1] The Osteoarthritis Initiative is a public-private partnership comprised of five contracts (N01-AR-2-2258; N01-AR-2-2259; N01-AR-2-2260; N01-AR-2-2261; N01-AR-2-2262) funded by the National Institutes of Health, a branch of the Department of Health and Human Services, and conducted by the OAI Study Investigators. Private funding partners include Merck Research Laboratories; Novartis Pharmaceuticals Corporation, GlaxoSmithKline; and Pfizer, Inc. Private sector funding for the OAI is managed by the Foundation for the National Institutes of Health. This manuscript was prepared using an OAI public use data set and does not necessarily reflect the opinions or views of the OAI investigators, the NIH, or the private funding partners.

15. Fletcher, P., Lu, C., Pizer, S., Joshi, S.: Principal geodesic analysis for the study of nonlinear statistics of shape. IEEE Trans Med Imaging **23**(8), 995–1005 (2004)
16. Freifeld, O., Black, M.J.: Lie bodies: A manifold representation of 3d human shape. In: ECCV. pp. 1–14. Springer (2012)
17. Fuchs, M., Jüttler, B., Scherzer, O., Yang, H.: Shape metrics based on elastic deformations. J Math Imaging Vis **35**(1), 86–102 (2009)
18. Gao, L., Lai, Y.K., Liang, D., Chen, S.Y., Xia, S.: Efficient and flexible deformation representation for data-driven surface modeling. ACM Trans Graph **35**(5), 158 (2016)
19. Hasler, N., Stoll, C., Sunkel, M., Rosenhahn, B., Seidel, H.P.: A statistical model of human pose and body shape. Comput Graph Forum **28**(2), 337–346 (2009)
20. Heeren, B., Zhang, C., Rumpf, M., Smith, W.: Principal geodesic analysis in the space of discrete shells. Comput Graph Forum **37**(5), 173–184 (2018)
21. Hefny, M.S., Okada, T., Hori, M., Sato, Y., Ellis, R.E.: A liver atlas using the special Euclidean group. In: MICCAI. pp. 238–245. Springer (2015)
22. Heimann, T., Meinzer, H.P.: Statistical shape models for 3d medical image segmentation: A review. Med Image Anal **13**(4), 543–563 (2009)
23. Joshi, S., Davis, B., Jomier, M., Gerig, G.: Unbiased diffeomorphic atlas construction for computational anatomy. NeuroImage **23**, S151–S160 (2004)
24. Kircher, S., Garland, M.: Free-form motion processing. ACM Trans Graph **27**(2), 12 (2008)
25. Rumpf, M., Wirth, B.: An elasticity-based covariance analysis of shapes. Int J Comput Vis **92**(3), 281–295 (2011)
26. von Tycowicz, C., Ambellan, F., Mukhopadhyay, A., Zachow, S.: An efficient Riemannian statistical shape model using differential coordinates. Med Image Anal **43**, 1–9 (2018)
27. von Tycowicz, C., Schulz, C., Seidel, H.P., Hildebrandt, K.: Real-time nonlinear shape interpolation. ACM Trans Graph **34**(3), 34:1–34:10 (2015)
28. Zhang, C., Heeren, B., Rumpf, M., Smith, W.A.: Shell PCA: Statistical shape modelling in shell space. In: ICCV. pp. 1671–1679. IEEE (2015)